Multi-insertion Reactions of Isocyanides with Zirconium Amido Silyl Complexes

Zhongzhi Wu, Jonathan B. Diminnie, and Ziling Xue*

Department of Chemistry, The University of Tennessee, Knoxville, Tennessee 37996-1600

Received December 3, 1998

The reactions of $(Me_2N)_3ZrSi(SiMe_3)_3$ (**1**), $(Me_2N)_3ZrSiPh_2Bu^t(THF)_{0.5}$ (**2**), and $(Me_2N)_2[(Me_3Si)_2N]ZrSi(SiMe_3)_3$ (**3**) with 2,6-dimethylphenyl isocyanide (ArNC) or *tert*-butyl isocyanide (Bu^tNC) have been investigated. The first ArNC was found to insert exclusively into the *Zr−Si* bond in complex **3** and, in contrast, into the *Zr−N* bonds in complex **1**. Up to 4 equiv of ArNC react with **1** and **2** to give $(Me_2N)_2Zr[Si(SiMe_3)_3][\eta^2\text{-}C(NMe_2)=NAr]$ (**4**), $(Me_2N)Zr[Si(SiMe_3)_3][\eta^2\text{-}C(NMe_2)=NAr]_2$ (**5**), $(Me_2N)Zr[\eta^2\text{-}C(NMe_2)=NAr]_2\{\eta^2\text{-}C[Si(SiMe_3)_3]=NAr\}$ (**6**), $Zr[\eta^2\text{-}C(NMe_2)=NAr]_3\{\eta^2\text{-}C[Si(SiMe_3)_3]=NAr\}$ (**7**), and $Zr[\eta^2\text{-}C(NMe_2)=NAr]_3[\eta^2\text{-}C(SiPh_2Bu^t)=NAr]$ (**8**). However, **3** reacts with only 2 equiv of ArNC to yield $(Me_2N)_2[(Me_3Si)_2N]Zr\{\eta^2\text{-}C[Si(SiMe_3)_3]=NAr\}$ (**9**) and $(Me_2N)[(Me_3Si)_2N]Zr[\eta^2\text{-}C(NMe_2)=NAr]\{\eta^2\text{-}C[Si(SiMe_3)_3]=NAr\}$ (**10**). Complex **2** was found to react with 2 equiv of Bu^tNC to yield a ketenimine complex $(Me_2N)_3Zr[N(Bu^t)C(SiPh_2Bu^t)=C=NBu^t]$ (**12**). The reactions of $Zr(NMe_2)_4$ with ArNC and Bu^tNC were also studied and gave tetrainsertion products $Zr[\eta^2\text{-}C(NMe_2)=NR]_4$ [R = Bu^t (**13**), 2,6-dimethylphenyl (**14**)]. The structures of **7**, **12**, **13**, and **14** have been determined by X-ray crystallography.

Introduction

Early-transition-metal d^0 silyl chemistry has attracted special attention in the past decade.[1,2] Group 4 d^0 metal silyl complexes were found to undergo insertion and σ-bond metathesis reactions involving M−Si bonds.[2a−c,k,3−6] However, reactivity studies of d^0 metal silyl complexes have been mainly concentrated on those containing π-anionic auxiliary ligands such as η^5-cyclopentadienyl (Cp).[1,2] The chemistry of Cp-free d^0 metal silyl complexes is a relatively young and unexplored area. The research interests in our laboratory have recently been focused on the chemistry of Cp-free d^0 early-transition-metal complexes, such as alkyl silyl[7] and amido silyl complexes.[8] These electronically and coordinatively unsaturated complexes present a new and unique opportunity to directly compare the relative reactivities of alkyl, amido, and silyl ligands.

We reported recently that in the reactions of alkyl silyl complexes $(Me_3ECH_2)_3ZrSi(SiMe_3)_3$ with ArNC, the first isocyanide insertion occurred exclusively into the

(1) (a) Tilley, T. D. In *The Chemistry of Organic Silicon Compounds*; Patai, S., Rappoport, Z.; Eds.; Wiley: New York, 1989; Chapter 24. (b) Tilley, T. D. In *The Silicon-Heteroatom Bond*; Patai, S., Rappoport, Z., Eds.; Wiley: New York, 1991; Chapter 9 and 10. (c) Tilley, T. D. *Comments Inorg. Chem*. **1990**, *10*, 37. (d) Harrod, J. F.; Mu, Y.; Samuel, E. *Polyhedron* **1991**, *11*, 1239. (e) Corey, J. Y. In *Advances in Silicon Chemistry*; Larson, G., Ed.; JAI Press: Greenwich, CT, 1991; Vol. 1, p 327. (f) Xue, Z. *Comments Inorg. Chem*. **1996**, *18*, 223. (g) Tilley, T. D. *Acc. Chem. Res*. **1993**, *26*, 22. (h) Sharma, H. K.; Pannell, K. H. *Chem. Rev*. **1995**, *95*, 1351.

(2) (a) Woo, H.-G.; Walzer, J. F.; Tilley, T. D. *J. Am. Chem. Soc*. **1992**, *114*, 7047. (b) Imori, T.; Tilley, T. D. *Polyhedron* **1994**, *13*, 2231. (c) Radu, N. S.; Engeler, M. P.; Gerlach, C. P.; Tilley, T. D.; Rheingold, A. L. *J. Am. Chem. Soc*. **1995**, *117*, 3621. (d) Xin, S. X.; Harrod, J. F. *J. Organomet. Chem*. **1995**, *499*, 181. (e) Dioumaev, V. K.; Harrod, J. F. *J. Organomet. Chem*. **1996**, *521*, 133. (f) Dioumaev, V. K.; Harrod, J. F. *Organometallics* **1996**, *15*, 3859. (g) Hao, L. J.; Lebuis, A. M.; Harrod, J. F.; Samuel, E. *J. Chem. Soc., Chem. Commun*. **1997**, 2193. (h) Dioumaev, V. K.; Harrod, J. F. *Organometallics* **1997**, *16*, 2798. (i) Jiang, Q.; Pestana, D. C.; Carroll, P. J.; Berry, D. H. *Organometallics* **1994**, *13*, 3679. (j) Procopio, L. J.; Carroll, P. J.; Berry, D. H. *Polyhedron* **1995**, *14*, 45. (k) Corey, J. Y.; Rooney, S. M. *J. Organomet. Chem*. **1996**, *521*, 75. (l) Shaltout, R. M.; Corey, J. Y. *Organometallics* **1996**, *15*, 2866. (m) Huhmann, J. L.; Corey, J. Y.; Rath, N. P. *J. Organomet. Chem*. **1997**, *533*, 61. (n) Hengge, E.; Gspaltl, P.; Pinter, E. *J. Organomet. Chem*. **1996**, *521*, 145. (o) Banovetz, J. P.; Suzuki, H.; Waymouth, R. M. *Organometallics* **1993**, *12*, 4700. (p) Spaltenstein, E.; Palma, P.; Kreutzer, K. A.; Willoughby, C. A.; Davis, W. M.; Buchwald, S. L. *J. Am. Chem. Soc*. **1994**, *116*, 10308. (q) Verdaguer, X.; Lange, U. E. W.; Reding, M. T.; Buchwald, S. L. *J. Am. Chem. Soc*. **1996**, *118*, 6784. (r) Fu, P. F.; Marks, T. J. *J. Am. Chem. Soc*. **1995**, *117*, 10747. (s) Schumann, H.; Meese-Marktscheffel, J. A.; Hahn, F. E. *J. Organomet. Chem*. **1990**, *390*, 301. (t) Molander, G. A.; Nichols, P. J. *J. Am. Chem. Soc*. **1995**, *117*, 4415. (u) Takahashi, T.; Hasegawa, M.; Suzuki, N.; Saburi, M.; Rousset, C. J.; Fanwick, P. E.; Negishi, E. *J. Am. Chem. Soc*. **1991**, *113*, 8564.

(3) (a) Tilley, T. D. *J. Am. Chem. Soc*. **1985**, *107*, 4084. (b) Campion, B. K.; Falk, J.; Tilley, T. D. *J. Am. Chem. Soc*. **1987**, *109*, 2049. (c) Elsner, F. H.; Woo, H.-G.; Tilley, T. D. *J. Am. Chem. Soc*. **1988**, *110*, 313. (d) Arnold, J.; Engeler, M. P.; Elsner, F. H.; Heyn, R. H.; Tilley, T. D. *Organometallics* **1989**, *8*, 2284. (e) Elsner, F. H.; Tilley, T. D.; Rheingold, A. L.; Geib, S. *J. Organomet. Chem*. **1988**, *358*, 169. (f) Heyn, R. H.; Tilley, T. D. *Inorg. Chem*. **1989**, *28*, 1768.

(4) Procopio, L. J.; Carroll, P. J.; Berry, D. H.*Organometallics* **1993**, *12*, 3087.

(5) (a) Aitken, C. T.; Harrod, J. F.; Samuel, E. *J. Am. Chem. Soc*. **1986**, *108*, 4059. (b) Aitken, C. T.; Barry, J.-P.; Gauvin, F.; Harrod, J. F.; Malek, A.; Rousseau, D. *Organometallics* **1989**, *8*, 1732. (c) Mu, Y.; Aitken, C. T.; Cote, B.; Harrod, J. F.; Samuel, E. *Can. J. Chem*. **1991**, *69*, 264. (d) Harrod, J. F. In *Inorganic and Organometallic Polymers with Special Properties* (NATO ASI Series E, Vol. 206); Laine, R. M., Ed.; Kluwer Academic Publishers: Amsterdam, 1991; p 87.

(6) (a) Corey, J. Y.; Zhu, X. H. *Organometallics* **1992**, *11*, 672. (b) Kesti, M. R.; Waymouth, R. M. *Organometallics* **1992**, *11*, 1095.

(7) (a) Xue, Z.; Li, L.; Hoyt, L. K.; Diminnie, J. B.; Pollitte, J. L. *J. Am. Chem. Soc*. **1994**, *116*, 2169. (b) McAlexander, L. H.; Hung, M.; Li, L.; Diminnie, J. B.; Xue, Z.; Yap, G. P. A.; Rheingold, A. L. *Organometallics* **1996**, *15*, 5231. (c) Diminnie, J. B.; Hall, H. D.; Xue, Z. *J. Chem. Soc., Chem. Commun*. **1996**, 2383. (d) Li, L.; Diminnie, J. B.; Liu, X.; Pollitte, J. L.; Xue, Z. *Organometallics* **1996**, *15*, 3520. (e) Diminnie, J. B.; Xue, Z. *J. Am. Chem. Soc*. **1997**, *119*, 12657. (f) Wu, Z.; Diminnie, J. B.; Xue, Z. *Organometallics* **1998**, *17*, 2917. (g) Liu, X.; Li, L.; Diminnie, J. B.; Yap, G. P. A.; Rheingold, A. L.; Xue, Z. *Organometallics* **1998**, *17*, 4597. (h) Chen, T.; Wu, Z.; Li, L.; Sorasaenee, K. R.; Diminnie, J. B.; Pan, H.; Guzei, I. A.; Rheingold, A. L.; Xue, Z. *J. Am. Chem. Soc*. **1998**, *120*, 13519.

(8) Wu, Z.; Diminnie, J. B.; Xue, Z. *Inorg. Chem*. **1998**, *37*, 6366.

10.1021/om980979l CCC: $18.00
Publication on Web 02/24/1999

Scheme 1

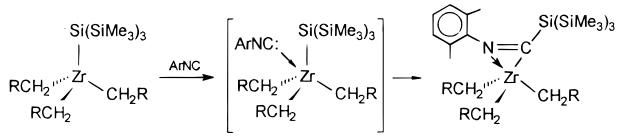

R = Me_3C, Me_3Si; Ar = 2,6-dimethylphenyl

Zr−Si bonds (Scheme 1).[9] This preferential isocyanide insertion into the Zr−Si bonds in the alkyl silyl system prompted us to study the reactions of the amido analogues $(Me_2N)_3ZrSiR_3$ [SiR_3 = $Si(SiMe_3)_3$ (**1**), $SiPh_2Bu^t$ (**2**)] and $(Me_2N)_2[(Me_3Si)_2N]ZrSi(SiMe_3)_3$ (**3**) with isocyanide. Insertions of isocyanides (RNC) into M−C,[10−16] M−N,[10,17] and M−Si[3,18] bonds of early-transition-metal complexes are well documented; however, there are only a few reports of the reactions of isocyanides with metal complexes containing different reactive ligands.[3e,9,19] The reactions of isocyanides with complexes involving both M−Si and M−N bonds, to our knowledge, have not been investigated. Our amido silyl complexes **1**−**3** offer a unique opportunity to observe the direct competition between silyl and amido ligands in the migration step and to study whether silyl or amido ligand migration is preferred. In this paper, we report our investigations of the reactions of isocyanides with $(Me_2N)_3ZrSi(SiMe_3)_3$ (**1**), $(Me_2N)_3ZrSiPh_2Bu^t(THF)_{0.5}$ (**2**), and $(Me_2N)_2[(Me_3Si)_2N]ZrSi(SiMe_3)_3$ (**3**).

Experimental Section

General Procedures. All manipulations were performed under a dry nitrogen atmosphere with the use of either standard Schlenk techniques or a glovebox. Solvents were purified by distillation over potassium/benzophenone ketyl. Benzene-d_6 was dried over activated molecular sieves and stored under nitrogen. 2,6-Dimethylphenyl isocyanide (Fluka) and Bu^tNC (Aldrich) were used as received. $(Me_2N)_3ZrSi(SiMe_3)_3$ (**1**), $(Me_2N)_3ZrSiPh_2Bu^t{\cdot}THF_{0.5}$ (**2**), and $(Me_2N)_2[(Me_3Si)_2N]ZrSi(SiMe_3)_3$ (**3**) were prepared by the reactions of $(Me_2N)_3ZrCl$ or $(Me_2N)_2[(Me_3Si)_2N]ZrCl$ with the corresponding silyllithium reagents.[8] NMR spectra were recorded on a Bruker AC-250 Fourier transform spectrometer and referenced to solvents (residual protons in the ^1H spectra). Elemental analyses were performed by E+R Microanalytical Laboratory, Corona, NY.

$(Me_2N)Zr[\eta^2\text{-}C(NMe_2){=}NAr]_2\{\eta^2\text{-}C[Si(SiMe_3)_3]{=}NAr\}$ (6). To a pale yellow solution of **1** (0.50 g, 1.06 mmol) in 20 mL of pentane at −20 °C was added dropwise 2,6-dimethylphenyl isocyanide (0.42 g, 3.18 mmol) in 20 mL of pentane with vigorous stirring. The reaction solution rapidly turned bright yellow. After stirring at room temperature overnight, the reaction solution was concentrated and slowly cooled to −18 °C to yield 0.86 g of **6** as a pale yellow solid (94% yield). ^1H NMR (benzene-d_6, 250 MHz, 23 °C): δ 6.93−6.86 (m, 9H, C_6H_3), 3.06 (s, 6H, $ZrNMe_2$), 2.92 (s, 6H, $N{=}CNMe_2$), 2.22 (s, 6H, $N{=}CNMe_2$), 2.05 (s, 6H, $C_6H_3Me_2$), 2.03 (s, 6H, $C_6H_3Me_2$), 1.96 (s, 6H, $C_6H_3Me_2$), 0.31 [s, 27H, $Si(SiMe_3)_3$]. $^{13}C\{^1H\}$ NMR (benzene-d_6, 62.9 MHz, 23 °C): δ 297.1 [$N{=}CSi(SiMe_3)_3$], 211.6 ($N{=}CNMe_2$), 156.6, 150.2, 131.5, 131.2, 128.6, 127.4, 124.9, 123.4 (C_6H_3), 46.7 ($N{=}CNMe_2$), 45.9 ($ZrNMe_2$), 36.1 ($N{=}CNMe_2$), 19.4 ($C_6H_3Me_2$), 19.0 ($C_6H_3Me_2$), 2.8 [$Si(SiMe_3)_3$]. Anal. Calcd for $C_{42}H_{72}N_6Si_4Zr$: C, 58.34; H, 8.39. Found: C, 58.50; H, 8.50.

$Zr[\eta^2\text{-}C(NMe_2){=}NAr]_3\{\eta^2\text{-}C[Si(SiMe_3)_3]{=}NAr\}$ (7). To a pale yellow solution of **1** (0.50 g, 1.06 mmol) in hexanes (20 mL) was added dropwise with stirring 0.56 g (4.24 mmol) of 2,6-dimethylphenyl isocyanide in hexanes (20 mL) at room temperature. The bright yellow solution was allowed to stir overnight at room temperature. The solution was then filtered, concentrated to about 5 mL, and slowly cooled to −20 °C to give 1.00 g of **7** as yellow crystals (95% yield). ^1H NMR (benzene-d_6, 250 MHz, 23 °C): δ 8.90, 6.88 (d, 12H, C_6H_3), 2.89 (s, 9H, $N{=}CNMe_2$), 2.20 (s, 9H, $N{=}CNMe_2$), 1.96 (s, 6H, $C_6H_3Me_2$), 1.94 (s, 18H, $C_6H_3Me_2$), 0.27 [s, 27H, $Si(SiMe_3)_3$]. $^{13}C\{^1H\}$ NMR (benzene-d_6, 62.9 MHz, 23 °C): δ 291.4 [$N{=}CSi(SiMe_3)_3$], 212.3 ($N{=}CNMe_2$), 156.4, 151.2, 131.7, 129.2, 128.7, 127.5, 124.8, 123.0 (C_6H_3), 47.0 ($N{=}CNMe_2$), 36.6 ($N{=}CNMe_2$), 20.3 ($C_6H_3Me_2$), 20.0 ($C_6H_3Me_2$), 3.9 [$Si(SiMe_3)_3$]. Anal. Calcd for $C_{51}H_{81}N_7Si_4Zr$: C, 61.51; H, 8.20. Found: C, 61.45; H, 8.40.

$Zr[\eta^2\text{-}C(NMe_2){=}NAr]_3[\eta^2\text{-}C(SiPh_2Bu^t){=}NAr]$ (8). Complex **2** (0.10 g, 0.20 mmol) and 2,6-dimethylphenyl isocyanide (0.11 g, 0.84 mmol) were placed into a Schlenk tube and dissolved in 5 mL of benzene at room temperature to give a yellow-orange solution. After 30 min, the solvent was removed, and the yellow solid was redissolved in 5 mL of pentane. The solution was concentrated and cooled to −18 °C to afford 0.15 g of yellow microcrystalline **8** (73% yield). ^1H NMR (benzene-d_6, 250 MHz, 23 °C): δ 7.52−6.50 (m, 22H, C_6H_5, C_6H_3), 2.85 (s, 9H, $N{=}CNMe_2$), 2.22 (s, 9H, $N{=}CNMe_2$), 1.98 (s, 18H, $C_6H_3Me_2$), 1.77 (s, 6H, $C_6H_3Me_2$), 1.28 (s, 9H, $SiPh_2Bu^t$). $^{13}C\{^1H\}$ NMR (benzene-d_6, 62.9 MHz, 23 °C): δ 292.9 ($N{=}CSiPh_2Bu^t$), 212.7 ($N{=}CN$), 154.1, 151.4, 137.2, 135.5, 131.7, 128.8, 128.5, 127.8, 127.5, 127.1, 124.6, 123.0 (C_6H_5, C_6H_3), 46.5 ($N{=}CNMe_2$), 36.5 ($N{=}CNMe_2$), 29.3 ($SiPh_2CMe_3$), 20.1 ($SiPh_2CMe_3$), 19.9 ($SiC{=}NC_6H_3Me_2$), 19.7 ($NC{=}NC_6H_3Me_2$). Anal. Calcd for $C_{58}H_{73}N_7SiZr$: C, 70.54; H, 7.45. Found: C, 70.31; H, 7.37.

$(Me_2N)[(Me_3Si)_2N]Zr[\eta^2\text{-}C(NMe_2){=}NAr]\{\eta^2\text{-}C[Si(SiMe_3)_3]{=}NAr\}$ (10). To a pale yellow solution of **3** (0.11 g, 0.18 mmol) in benzene was added 2 equiv of 2,6-dimethylphe-

(9) Wu, Z.; McAlexander, L. H.; Diminnie, J. B.; Xue, Z. *Organometallics* **1998**, *17*, 4853.
(10) Durfee, L. D.; Rothwell, I. P. *Chem. Rev.* **1988**, *88*, 1059, and references therein.
(11) (a) Lappert, M. F.; Luong-Thi, N. T.; Milne, C. R. C. *J. Organomet. Chem.* **1979**, *174*, C35. (b) Wolczanski, P. T.; Bercaw, J. E. *J. Am. Chem. Soc.* **1979**, *101*, 6450. (c) Chiu, K. W.; Jones, R. A.; Wilkinson, G.; Galas, A. M. R.; Hursthouse, M. B. *J. Chem. Soc., Dalton Trans.* **1981**, 2088. (d) Negishi, E.; Swanson, D. R.; Miller, S. R. *Tetrahedron Lett.* **1988**, *29*, 1631. (e) Buchwald, S. L.; Nielsen, R. B. *Chem. Rev.* **1988**, *88*, 1047. (f) Lyszak, E. L.; O'Brien, J. P.; Kort, D. A.; Hendges, S. K.; Redding, R. N.; Bush, T. L.; Hermen, M. S.; Renkema, K. B.; Silver, M. E.; Huffman, J. C. *Organometallics* **1993**, *12*, 338. (g) Aoyagi, K.; Kasai, K.; Kondakov, D. Y.; Hara, R.; Suzuki, N.; Takahashi, T. *Inorg. Chim. Acta* **1994**, *220*, 319. (h) Barriola, A. M.; Cano, A. M.; Cuenca, T.; Fernandez, F. J.; Gomez-Sal, P.; Manzanero, A.; Royo, P. *J. Organomet. Chem.* **1997**, *542*, 247.
(12) (a) Stockman, K. E.; Houseknecht, K. L.; Boring, E. A.; Sabat, M.; Finn, M. G.; Grimes, R. N. *Organometallics* **1995**, *14*, 3014. (b) Houseknecht, K. L.; Stockman, K. E.; Sabat, M.; Finn, M. G.; Grimes, R. N. *J. Am. Chem. Soc.* **1995**, *117*, 1163. (c) Boring, E.; Sabat, M.; Finn, M. G.; Grimes, R. N. *Organometallics* **1997**, *16*, 3993.
(13) (a) Chamberlain, L. R.; Durfee, L. D.; Fanwick, P. E.; Kobriger, L.; Latesky, S. L.; McMullen, A. K.; Rothwell, I. P.; Folting, K.; Huffman, J. C.; Streib, W. E.; Wang, R. *J. Am. Chem. Soc.* **1987**, *109*, 390. (b) Chamberlain, L. R.; Durfee, L. D.; Fanwick, P. E.; Kobriger, L.; Latesky, S. L.; McMullen, A. K.; Rothwell, I. P.; Folting, K.; Huffman, J. C.; Streib, W. E. *J. Am. Chem. Soc.* **1987**, *109*, 6068.
(14) Kloppenburg, L.; Petersen, J. L.*Organometallics* **1997**, *16*, 3548, and references therein.
(15) Scott, M. J.; Lippard, S. J. *Organometallics* **1997**, *16*, 5857.
(16) Giannini, L.; Caselli, A.; Solari, E.; Floriani, C.; Chiesi-Villa, A.; Rizzoli, C.; Re, N.; Sgamellotti, A. *J. Am. Chem. Soc.* **1997**, *119*, 9709.
(17) (a) Chisholm, M. H.; Hammond, C. E.; Huffman, J. C. *Organometallics* **1987**, *6*, 210. (b) Chisholm, M. H.; Hammond, C. E.; Ho, D.; Huffman, J. C. *J. Am. Chem. Soc.* **1986**, *108*, 7860. (c) Lappert, M. F.; Power, P. P.; Sanger, A. R.; Srivastava, R. C. *Metal and Metalloid Amides*; Ellis Horwood Limited: Chichester, U.K., 1980; Chapter 10.
(18) (a) Casty, G. L.; Tilley, T. D.; Yap, G. P. A.; Rheingold, A. L. *Organometallics* **1997**, *16*, 4746. (b) Arnold, J.; Tilley, T. D.; Rheingold, A. L.; Geib, S. J.; Arif, A. M. *J. Am. Chem. Soc.* **1989**, *111*, 149. (c) Campion, B. K.; Heyn, R. H.; Tilley, T. D. *Organometallics* **1993**, *12*, 2584. (d) Honda, T.; Satoh, S.; Mori, M. *Organometallics* **1995**, *14*, 1548.
(19) (a) Anderson, R. A. *Inorg. Chem.* **1979**, *18*, 2928. (b) Dormond, A.; Aaliti, A.; Moise, C. *J. Chem. Soc., Chem. Commun.* **1985**, 1231.

Table 1. Crystallographic Data for 7, 12, 13, and 14

	7	12	13	14
formula	$C_{51}H_{81}N_7Si_4Zr$	$C_{32}H_{55}N_5SiZr$	$C_{28}H_{60}N_8Zr$	$C_{44}H_{60}N_8Zr$
cryst size, mm^3	0.40 × 0.20 × 0.20	0.50 × 0.44 × 0.40	0.46 × 0.42 × 0.42	0.62 × 0.50 × 0.50
T, K	173(2)	173(2)	173(2)	173(2)
cryst syst	triclinic	monoclinic	tetragonal	triclinic
space group	$P\bar{1}$	$P2_1/c$	$I\bar{4}$	$P\bar{1}$
a, Å	10.980(4)	12.136(6)	13.053(3)	11.380(3)
b, Å	15.015(6)	17.126(7)	13.053(3)	12.240(3)
c, Å	16.995(7)	17.217(8)	7.790(4)	16.703(5)
α, deg	90.13(3)	90	90	94.49(3)
β, deg	95.08(3)	99.45(3)	90	96.45(3)
γ, deg	97.48(3)	90	90	112.09(2)
V, Å^3	2767(2)	3530(3)	1668.0(9)	2123.7(10)
Z	2	4	2	2
fw	995.81	629.12	600.2	792.22
$d_{calc.}$, g/cm^3	1.195	1.184	1.195	1.239
μ, mm^{-1}	0.324	0.372	0.358	0.299
F(000)	1064	1344	648	840
scan type	$\omega-2\theta$	$\omega-2\theta$	$\omega-2\theta$	$\omega-2\theta$
θ range, deg	1.81−22.55	1.69−22.57	2.21−22.51	1.81−25.05
no. of data [$I > 2\sigma(I)$]	7257	4647	642	7501
abs corr	semiempirical	semiempirical	semiempirical	semiempirical
$R1$[a] (w$R2$)[b]	0.0920(0.1408)	0.0593(0.1136)	0.0301(0.0780)	0.0483(0.1272)
GOF	1.093	1.098	1.136	1.076
no. of variables	568	352	84	478
$\rho_{max,min}$ (e Å^{-3})	0.489, −0.475	0.403, −0.371	0.343, −0.284	0.561, −0.476

[a] $R1 = \sum||F_o| - |F_c||/\sum|F_o|$. [b] $wR2 = (\sum[w(F_o^2 - F_c^2)^2]/\sum[w(F_o^2)^2)^{1/2}$.

nyl isocyanide (0.05 g, 0.37 mmol) at room temperature. The bright yellow reaction solution was allowed to stand at room temperature for 24 h. The solvent was then removed in vacuo to give a bright yellow solid, which was redissolved in pentane. The pentane solution was concentrated and slowly cooled to −18 °C to yield bright yellow crystals of **10** (0.11 g, 71% yield). ^{1}H NMR (benzene-d_6, 250 MHz, 23 °C): δ 6.92−6.85 (m, 6H, C_6H_3), 2.88 (s, 6H, ZrNMe_2), 2.84 (s, 3H, N=CNMe_2), 2.18 (s, 3H, N=CNMe_2), 2.14 (s, 3H, $C_6H_3Me_2$), 2.05 (s, 3H, $C_6H_3Me_2$), 1.89 (s, 3H, $C_6H_3Me_2$), 1.76 (s, 3H, $C_6H_3Me_2$), 0.39 (s, 18H, N(SiMe_3)$_2$], 0.30 [s, 27H, Si(SiMe_3)$_3$]. ^{13}C{^{1}H} NMR (benzene-d_6, 62.9 MHz, 23 °C): δ 295.8 [N=*C*Si(SiMe$_3$)$_3$], 207.6 (N=*C*NMe$_2$), 154.9, 149.3, 131.8, 131.6, 127.7, 127.5, 125.5, 124.2 (C_6H_3), 46.4 (N=CNMe_2), 44.1 (ZrNMe_2), 36.7 (N=CNMe_2), 19.9 ($C_6H_3Me_2$), 19.5 ($C_6H_3Me_2$), 19.3 ($C_6H_3Me_2$), 18.9 ($C_6H_3Me_2$), 6.6 [N(SiMe_3)$_2$], 3.6 [Si(SiMe_3)$_3$]. Anal. Calcd for $C_{37}H_{75}N_5Si_6Zr$: C, 52.30; H, 8.90. Found: C, 51.94; H, 8.61.

(Me$_2$N)$_3$Zr[NBu^{t}C(SiPh$_2$Bu^t)=C=NBu^t] (12). A solution of 0.27 g (0.53 mmol) of **2** in benzene was added to a solution of Bu^{t}NC (0.18 g, 2.13 mmol) in benzene at room temperature. The clear, bright yellow solution was then allowed to stand at room temperature for 30 min. The solvent was then removed to give a yellow solid. The solid was redissolved in pentane and slowly cooled to −18 °C to afford 0.30 g of **12** as pale yellow crystals (66% yield). ^{1}H NMR (benzene-d_6, 250 MHz, 23 °C): δ 8.05−7.22 (m, 10H, C_6H_5), 3.00 (s, 18H, ZrNMe_2), 1.31 (s, 9H, SiCMe_3), 1.23 (s, 9H, NCMe_3), 1.20 (s, 9H, NCMe_3). ^{13}C{^{1}H} NMR (benzene-d_6, 62.9 MHz, 23 °C) δ 182.2 (N=*C*=CSi), 137.3, 129.1, 127.7, 127.0 (C_6H_5), 64.4 (N=C=*C*Si), 58.5 (N*C*Me$_3$), 57.4 (N*C*Me$_3$), 42.9 (ZrNMe_2), 30.9 (NCMe_3), 30.5 (NCMe_3), 29.2 (SiCMe_3), 20.8 (Si*C*Me$_3$). Anal. Calcd for $C_{32}H_{55}N_5$SiZr: C, 61.09; H, 8.81. Found: C, 61.13; H, 8.82.

Formation of Zr[η^2-C(NMe$_2$)=NBu^t]$_4$ (13). To a pale yellow solution of Zr(NMe$_2$)$_4$ (30 mg, 0.11 mmol) in benzene-d_6 in an NMR tube was added 4 equiv of Bu^{t}NC (38 mg, 0.45 mmol) at room temperature. The solution was placed at room temperature in a drybox for 1 week to yield 53 mg of **13** as colorless crystals (78% yield). The crystals were found to be almost insoluble in aliphatic and aromatic solvents. The structural assignment was thus based on its elemental analysis and X-ray crystal structure. Anal. Calcd for $C_{28}H_{60}N_8Zr$: C, 56.05; H, 10.08. Found: C, 56.05; H, 9.90.

Formation of Zr[η^2-C(NMe$_2$)=NAr]$_4$ (14). (Me$_2$N)$_4$Zr (30 mg, 0.11 mmol) and 2,6-dimethylphenyl isocyanide (59 mg, 0.44 mmol) were placed in an NMR tube and dissolved in benzene-d_6 at room temperature. An instantaneous reaction was observed to give the tetrainsertion product **14** in almost quantitative yield as shown by NMR. The reaction solution was slowly evaporated at room temperature to give 65 mg of **14** as colorless crystals (73% yield). ^{1}H NMR (benzene-d_6, 250 MHz, 23 °C): δ 7.00, 6.93 (m, 12H, C_6H_3), 2.89 (s, 12H, N=CNMe_2), 2.25 (s, 12H, N=CNMe_2), 2.04 (s, 24H, $C_6H_3Me_2$). ^{13}C-{^{1}H} NMR (benzene-d_6, 62.9 MHz, 23 °C): δ 212.8 (N=*C*NMe$_2$), 151.5, 131.1, 127.5, 122.6 (C_6H_3), 46.4 (N=CNMe_2), 36.2 (N=CNMe_2), 19.1 (C_6H_3Me). Anal. Calcd for $C_{44}H_{60}N_8Zr$: C, 66.71; H, 7.63. Found: C, 66.83; H, 7.72.

X-ray Data Collection and Structural Analyses of 7, 12, 13, and 14. All crystal structures were determined on a Siemens R3m/V diffractometer equipped with a Nicolet LT-2 low-temperature device. Suitable crystals were coated with Paratone oil (Exxon) and mounted under a stream of nitrogen at −100 °C. The unit cell parameters and orientation matrix were determined from a least-squares fit of the orientation of at least 25 reflections obtained from a rotation photograph and an automatic peak search routine. The refined lattice parameters and other pertinent crystallographic information are given in Table 1.

Intensity data were measured with graphite-monochromated Mo Kα radiation (λ = 0.710 73 Å). Background counts were measured at the beginning and end of each scan with the crystal and counter kept stationary. The intensities of three standard reflections were measured after every 97 reflections. The intensity data were corrected for Lorentz and polarization effects and an empirical absorption correction based upon ψ scans.

The structures were solved by direct methods using the Siemens SHELXTL 93 (version 5.0) proprietary software package. All non-hydrogen atoms were refined anisotropically. All hydrogen atoms were placed in calculated positions and introduced into the refinement as fixed contributors with an isotropic U value of 0.08 Å^2.

Results and Discussion

Synthesis and Characterization of Insertion Products 4−14. The reaction of the amido silyl complex

Table 2. Selected ^{13}C NMR Data

complex	δ (N=*C*R)[a]	δ (N=*C*Si)	δ Si(Si*Me*$_3$)$_3$
$(Me_2N)_3ZrSi(SiMe_3)_3$ (**1**)[8]			5.1
$(Me_2N)_2[(Me_3Si)_2N]ZrSi(SiMe_3)_3$ (**3**)[8]			5.6
$(Me_2N)_2Zr[Si(SiMe_3)_3][\eta^2$-C(NMe$_2$)=NAr] (**4**)	208.8		5.6
$(Me_2N)Zr[Si(SiMe_3)_3][\eta^2$-C(NMe$_2$)=NAr$]_2$ (**5**)	205.2		6.3
$(Me_2N)Zr[\eta^2$-C(NMe$_2$)=NAr$]_2\{\eta^2$-C[Si(SiMe$_3$)$_3$]=NAr} (**6**)	211.6	297.1	2.8
$Zr[\eta^2$-C(NMe$_2$)=NAr$]_3\{\eta^2$-C[Si(SiMe$_3$)$_3$]=NAr} (**7**)	212.3	291.4	3.9
$Zr[\eta^2$-C(NMe$_2$)=NAr$]_3[\eta^2$-C(SiPh$_2$Bu^t)=NAr] (**8**)	212.7	292.9	
$(Me_2N)_2[(Me_3Si)_2N]Zr\{\eta^2$-C[Si(SiMe$_3$)$_3$]=NAr} (**9**)		287.8	3.1
$(Me_2N)[(Me_3Si)_2N]Zr[\eta^2$-C(NMe$_2$)=NAr$]_2\{\eta^2$-C[Si(SiMe$_3$)$_3$]=NAr} (**10**)	207.6	295.8	3.6
$(Me_2N)_3Zr[\eta^2$-C(SiPh$_2$Bu^t)=NBu^t] (**11**)		287.6	
$Zr[\eta^2$-C(NMe$_2$)=NAr$]_4$ (**14**)	212.8		
$Mo[\eta^2$-C(NMe$_2$)=NAr$]_4$[17b]	194, 213		
$Np_3Zr\{\eta^2$-C[Si(SiMe$_3$)$_3$]=NAr}[9]		296.0	2.6
$Ns_3Zr\{\eta^2$-C[Si(SiMe$_3$)$_3$]=NAr}[9]		297.5	2.4
$Np_2Zr[\eta^2$-C(Np)=NAr$]\{\eta^2$-C[Si(SiMe$_3$)$_3$]=NAr}[9]	259.9	295.5	2.9
$Ns_2Zr[\eta^2$-C(Ns)=NAr$]\{\eta^2$-C[Si(SiMe$_3$)$_3$]=NAr}[9]	257.7	297.5	2.6
$NpZr[\eta^2$-C(Np)=NAr$]_2\{\eta^2$-C[Si(SiMe$_3$)$_3$]=NAr}[9]	261.0	298.8	3.5
$NsZr[\eta^2$-C(Ns)=NAr$]_2\{\eta^2$-C[Si(SiMe$_3$)$_3$]=NAr}[9]	258.5	294.8	3.1
$Cp_2Sc\{\eta^2$-C[Si(SiMe$_3$)$_3$]=NAr}[18c]		299.07	2.89
$Cp_2Zr\{\eta^2$-C[Si(SiMe$_3$)$_3$]=NAr}Cl[3b]		267.6	3.30
CpCp*$Zr\{\eta^2$-C[Si(SiMe$_3$)$_3$]=NAr}Cl[3e]		272.40	4.24
$(Bu^tO)_3Zr\{\eta^2$-C[Si(SiMe$_3$)$_3$]=NAr}[3f]		299.01	2.24
$Cp_2Zr[\eta^2$-C(SiPh$_2$Bu^t)=NPh]Cl[18d]		269.7	
$Cp'_2Zr[\eta^2$-C(Me)=NAr$]_2$[14]	251.8		
$(2,6\text{-}Bu^t_2C_6H_3O)_2Zr[\eta^2$-C(CH$_2$Ph)=NAr](CH$_2$Ph)[13a]	246.3		
$(2,6\text{-}Bu^t_2C_6H_3O)_2Zr[\eta^2$-C(Me)=NAr$]_2$[13a]	245.2		

[a] R = alkyl or amido ligand; Np = Me_3CCH_2; Ns = Me_3SiCH_2; Ar = 2,6-dimethylphenyl.

$(Me_2N)_3ZrSi(SiMe_3)_3$ (**1**) with 4 equiv of 2,6-dimethylphenyl isocyanide (ArNC) proceeds instantaneously at room temperature to give the tetra-insertion product **7**. The mono-insertion and di-insertion intermediates **4** and **5** were detected as well by NMR, when 1 and 2 equiv of ArNC were added to **1** (Scheme 2).[20] However, **4** and **5** are not stable in solution, and over days the NMR spectra showed their decomposition to HSi(SiMe$_3$)$_3$ and unidentified products. Attempts to isolate pure mono- (**4**) and di-insertion (**5**) products were unsuccessful. The tri-insertion intermediate **6** was obtained by the reaction of **1** with 3 equivalents of isocyanide (Scheme 2). The reaction of ArNC with $(Me_2N)_3ZrSiPh_2Bu^t(THF)_{0.5}$ (**2**) is extremely rapid, and only the tetra-insertion product **8** was isolated.

In the reaction of **1** with ArNC, the first and second equivalents of isocyanide were found to insert into Zr−N bonds. The insertion products were identified by the presence of the characteristic ^{1}H and ^{13}C NMR resonances of the Zr−Si(Si*Me*$_3$)$_3$ moiety in **4** (0.46 and 5.6 ppm) and **5** (0.54 and 6.3 ppm) (see Table 2).[20] Both ^{1}H and ^{13}C NMR resonances of the Zr−Si(Si*Me*$_3$)$_3$ moiety in **4** and **5** are downfield shifted from those (0.39 and 5.1 ppm) in the precursor **1** (Table 2). In addition, the characteristic ^{13}C NMR resonances for the (η^2-ArN=*C*NMe$_2$) ligands in **4** and **5** are at 208.8 and 205.2 ppm, respectively, and are close to those reported for Mo[η^2-C(NMe$_2$)=NAr]$_4$.[17b] They are, however, upfield shifted from that of an iminosilaacyl ligand (ca. 295 ppm) (Table 2). The third and fourth equivalents of ArNC were found to insert into the Zr−Si and remaining Zr−N bond to form **6** and **7** (Scheme 2).

Scheme 2

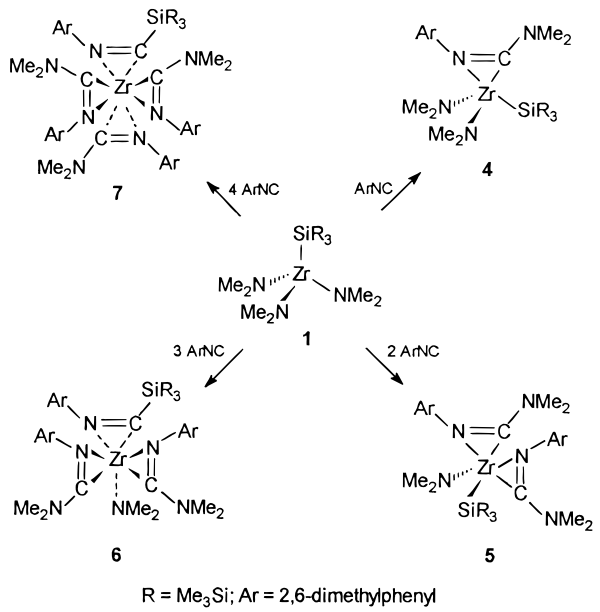

The reaction of ArNC with **3** is very fast at both room and low temperature. A di-insertion complex **10** was isolated and characterized. The NMR spectra of the di-insertion complex **10** show the characteristic ^{13}C NMR resonances of ArN=*C*Si and ArN=*C*NMe$_2$ at 295.8 and 207.6 ppm, respectively, and are similar to those in **4**−**8** (Table 2). The four 2,6-dimethylphenyl methyl groups of **10** are inequivalent in the ^{1}H NMR spectrum at 23 °C. This suggests a high degree of steric crowding in the molecule, leading to restricted rotations about the N−Ar bonds in **10**. This result is also consistent with

(20) NMR data for the mono-insertion complex $(Me_2N)_2Zr[Si(SiMe_3)_3][\eta^2$-C(NMe$_2$)=NAr] (**4**): ^{1}H NMR (benzene-d_6, 250 MHz, 23 °C) δ 6.93−6.86 (m, 3H, C$_6H_3$), 3.00 (s, 12H, ZrN*Me*$_2$), 2.90 (s, 3H, N=CN*Me*$_2$), 2.11 (s, 3H, N=CN*Me*$_2$), 2.00 (s, 6H, C$_6$H$_3$*Me*$_2$), 0.46 [s, 27H, Si(Si*Me*$_3$)$_3$]; ^{13}C{^{1}H} NMR (benzene-d_6, 62.9 MHz, 23 °C) δ 208.8 (N=*C*NMe$_2$), 148.9, 130.4, 128.9, 124.7 (*C*$_6$H$_3$), 44.7 (N=CN*Me*$_2$), 40.5 (ZrN*Me*$_2$), 36.2 (N=CN*Me*$_2$), 19.1 (C$_6$H$_3$*Me*$_2$), 5.6 [Si(Si*Me*$_3$)$_3$]. NMR data for di-insertion complex $(Me_2N)Zr[Si(SiMe_3)_3][\eta^2$-C(NMe$_2$)=NAr$]_2$ (**5**): ^{1}H NMR (benzene-d_6, 250 MHz, 23 °C) δ 6.93−6.86 (m, 6H, C$_6H_3$), 3.05 (s, 6H, ZrN*Me*$_2$), 3.03 (s, 6H, N=CN*Me*$_2$), 2.14 (s, 6H, N=CN*Me*$_2$), 2.00 (s, 6H, C$_6$H$_3$*Me*$_2$), 1.75 (s, 6H, C$_6$H$_3$*Me*$_2$), 0.52 [s, 27H, Si(Si*Me*$_3$)$_3$]; ^{13}C{^{1}H} NMR (benzene-d_6, 62.9 MHz, 23 °C) δ 205.2 (N=*C*NMe$_2$), 149.3, 130.6, 128.0, 124.4 (*C*$_6$H$_3$), 47.4 (N=CN*Me*$_2$), 42.7 (ZrN*Me*$_2$), 36.2 (N=CN*Me*$_2$), 19.6 (C$_6$H$_3$*Me*$_2$), 19.0 (C$_6$H$_3$*Me*$_2$), 6.3 [Si(Si*Me*$_3$)$_3$].

Scheme 3

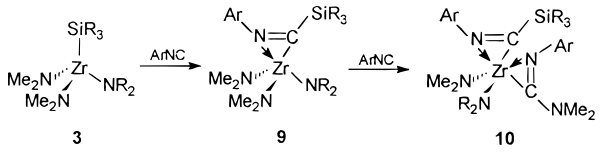

R = $SiMe_3$; Ar = 2,6-dimethylphenyl

Scheme 4

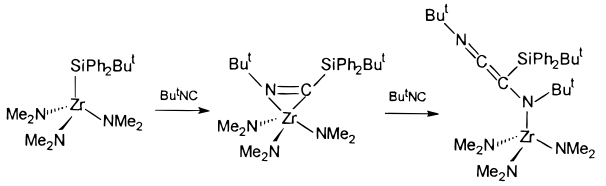

the fact that **10** is inert to further insertion by ArNC. Although it could not be isolated, the mono-insertion intermediate **9** was clearly identified in the reaction of **3** with ArNC.[21] The NMR data of **9** indicate that the insertion occurs first at the Zr−Si bond in the reaction of **3** with ArNC (Scheme 3) with the characteristic ^{13}C NMR of ArN=*C*Si in **9** at 287.8 ppm.

The reactions of **1** and **2** with ArNC are fast and difficult to control; we thus turned to the reactions of **1** and **2** with Bu^{t}NC. However, no reaction was observed between **1** and Bu^{t}NC at 23 °C over 1 day. The reaction of excess Bu^{t}NC with $(Me_2N)_3ZrSiPh_2Bu^t(THF)_{0.5}$ (**2**) resulted in an instantaneous formation of a red-orange solution, which rapidly changed to a pale yellow solution. From this solution, **12** was isolated as pale yellow crystals. An X-ray crystal structure determination revealed that **12** was a di-isocyanide addition product containing a ketenimine functionality. A possible mechanism for the formation of **12** is shown in Scheme 4. The insertion of Bu^{t}NC into the Zr−Si bond produces an η^2-iminosilaacyl **11**, which then undergoes nucleophilic addition of the second equivalent of Bu^{t}NC to form **12**. The di-isocyanide adduct **12** was found to be inert to further insertion by Bu^{t}NC. The intermediate **11** was observed by NMR.[22] Similar ketenimine complexes have been proposed, though not observed, as intermediates in the reactions of isocyanides with $Cp_2ScSi(SiMe_3)_3$,[18c] $(2,6\text{-}Pr^i_2C_6H_3O)_2Ta(H)Cl_2(PMe_2Ph)$,[23] and $[(Me_3Si)_2N]_2VMe(THF)$.[24] Recently, Scott and Lippard structurally characterized two ketenimine complexes {M(TC-3,3)[NBu^{t}C(CH_2Ph)=C=NBu^t]}(BPh_4) (M = Zr, Hf; TC = tropocoronand), prepared from alkyl complexes [M(TC-3,3)(CH_2Ph)](BPh_4) and 2 equiv of Bu^{t}NC.[25] **12**, to our knowledge, is the first structurally characterized ketenimine complex through isocyanide insertion to a M−silyl bond.

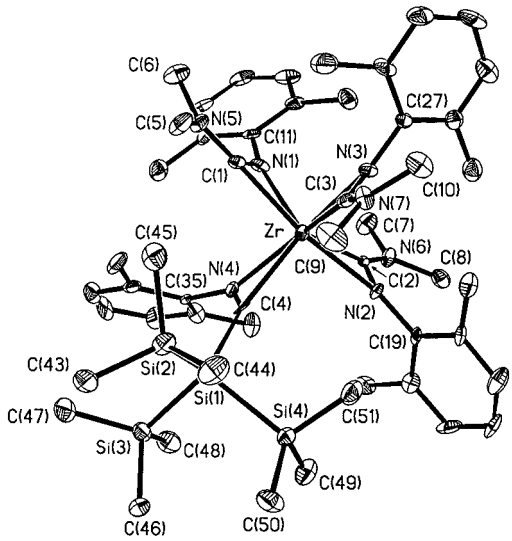

Figure 1. ORTEP drawing of Zr[η^2-C(NMe_2)=NAr]$_3${η^2-C[Si($SiMe_3$)$_3$]=NAr} (**7**), showing 35% thermal ellipsoids.

Scheme 5

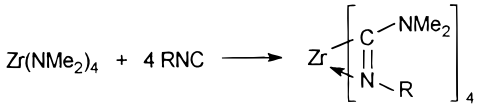

R = But. **13**: 2,6-dimethylphenyl. **14**

Although no insertion of Bu^{t}NC into the Zr−NMe_2 bonds was observed in the reaction of **2** with excess Bu^{t}NC, such insertion was observed in the reactions of Zr(NMe_2)$_4$ with excess Bu^{t}NC to give a tetra-insertion product Zr[η^2-C(NMe_2)=NBu^t]$_4$ (**13**) (Scheme 5). The reaction of Zr(NMe_2)$_4$ with Bu^{t}NC is very slow at room temperature, and **13** crystallizes from a benzene solution after a week. The reaction of Zr(NMe_2)$_4$ with 4 equiv of ArNC instantaneously gives a similar product, Zr[η^2-C(NMe_2)=NAr]$_4$ (**14**), at room temperature.

Molecular Structure of Zr[η^2-C(NMe_2)=NAr]$_3${η^2-C[Si($SiMe_3$)$_3$]=NAr} (7). The structure of **7** has been determined by X-ray crystallogaphy. An ORTEP drawing of **7** is shown in Figure 1. Selected bond distances and angles are listed in Table 3. Complex **7** contains one η^2-iminosilaacyl and three η^2-amidino ligands. The coordination sphere around the Zr atom can be described as a pseudotetrahedron with an η^2-C=N unit occupying a single coordination site. As seen in a simplified view of **7** in Figure 2, the iminosilaacyl and one of the amidino ligands [C(3)−N(3)] lie closely in a plane with carbon atoms cis to each other, and the other two amidino ligands arrange in another plane with carbon atoms trans to each other. These two planes are nearly perpendicular to each other with the C(1)−Zr−N(2) [167.3(3)°] and N(3)−Zr−N(4) [169.6(3)°] angles near 170°.

The Zr−N bond lengths [2.235(9)−2.310(8) Å] are similar to those in $(Me_3CCH_2)_3Zr${η^2-C[Si($SiMe_3$)$_3$]=NAr} [2.175(3) Å][9] and (Me_3CCH_2)Zr[η^2-C(CH_2CMe_3)=

(21) NMR data for the mono-insertion intermediate $(Me_2N)_2[(Me_3Si)_2N]Zr\{\eta^2\text{-}C[Si(SiMe_3)_3]=NAr\}$ (**9**): ^1H NMR (benzene-d_6, 250 MHz, 23 °C) δ 6.91 (s, 3H, C_6H_3), 2.97 (s, 12H, ZrNMe_2), 1.99 (s, 6H, $C_6H_3Me_2$), 0.34 [s, 18H, N(SiMe_3)$_2$], 0.24[s, 27H, Si(SiMe_3)$_3$]; $^{13}C\{^1H\}$ NMR (benzene-d_6, 62.9 MHz, 23 °C) δ 287.8 [N=*C*Si(SiMe_3)$_3$], 156.7, 129.1, 128.6, 125.9 (C_6H_3), 44.4 (ZrNMe_2), 19.5 ($C_6H_3Me_2$), 5.8 [N(SiMe_3)$_2$], 3.1 [Si(SiMe_3)$_3$].

(22) NMR data for the intermediate $(Me_2N)_3Zr[\eta^2\text{-}C(SiPh_2Bu^t)=NBu^t]$ (**11**): ^1H NMR (benzene-d_6, 250 MHz, 23 °C) δ 7.60, 7.17 (m, 10H, C_6H_5), 3.05 (s, 18H, ZrNMe_2), 1.36 (s, 9H, CMe_3), 1.15 [s, 9H, CMe_3]; $^{13}C\{^1H\}$ NMR (benzene-d_6, 62.9 MHz, 23 °C) δ 287.6 [N=*C*SiPh_2Bu^t], 136.7, 129.5, 128.2, 127.2 (C_6H_5), 56.9 (N*C*Me$_3$), 43.1 (ZrNMe_2), 30.1 (NCMe_3), 28.6(SiCMe_3), 19.4 (SiCMe_3).

(23) (a) Clark, J. R.; Fanwick, P. E.; Rothwell, I. P. *J. Chem. Soc., Chem. Commun.* **1993**, 1233. (b) Clark, J. R.; Fanwick, P. E.; Rothwell, I. P. *Organometallics* **1996**, *15*, 3232.

(24) Gerlach, C. P.; Arnold, J. *J. Chem. Soc., Dalton Trans.* **1997**, 4795.

(25) Scott, M. J.; Lippard, S. J. *Organometallics* **1998**, *17*, 1769.

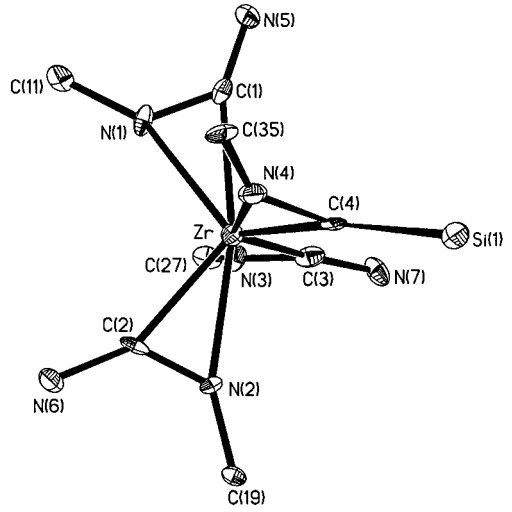

Figure 2. Simplified ORTEP drawing of the structure of $Zr[\eta^2\text{-}C(NMe_2)\text{=}NAr]_3\{\eta^2\text{-}C[Si(SiMe_3)_3]\text{=}NAr\}$ (**7**).

Table 3. Selected Bond Distances (Å) and Angles (deg) for 7

Distances			
Zr−C(1)	2.293(10)	C(1)−N(1)	1.308(12)
Zr−C(2)	2.240(10)	C(2)−N(2)	1.306(12)
Zr−C(3)	2.225(11)	C(3)−N(3)	1.301(13)
Zr−C(4)	2.347(10)	C(4)−N(4)	1.270(12)
Zr−N(1)	2.253(8)	C(4)−Si(1)	1.932(11)
Zr−N(2)	2.310(8)	Si(1)−Si(2)	2.396(5)
Zr−N(3)	2.285(9)	Si(1)−Si(3)	2.373(5)
Zr−N(4)	2.235(9)	Si(1)−Si(4)	2.362(5)
C(1)−N(5)	1.341(12)	N(4)−C(35)	1.441(12)
N(1)−C(11)	1.447(13)	C(2)−N(6)	1.361(12)
N(2)−C(19)	1.427(12)	C(3)−N(7)	1.365(13)
N(3)−C(27)	1.417(13)		

Angles			
Zr−C(1)−N(1)	71.6(6)	Zr−C(3)−N(3)	75.8(6)
Zr−C(1)−N(5)	158.0(8)	Zr−C(3)−N(7)	157.8(8)
Zr−N(1)−C(1)	74.9(6)	Zr−N(3)−C(3)	70.7(6)
Zr−N(1)−C(11)	154.0(7)	Zr−N(3)−C(27)	156.5(7)
Zr−C(2)−N(2)	76.3(6)	Zr−C(4)−N(4)	69.1(6)
Zr−C(2)−N(6)	153.7(8)	Zr−C(4)−Si(1)	160.5(6)
Zr−N(2)−C(2)	70.4(6)	Zr−N(4)−C(4)	78.8(6)
Zr−N(2)−C(19)	158.0(7)	Zr−N(4)−C(35)	148.9(7)
N(1)−Zr−N(2)	134.9(3)	N(3)−Zr−N(4)	169.6(3)
N(1)−Zr−N(3)	92.1(3)	N(3)−Zr−C(1)	88.2(3)
N(1)−Zr−N(4)	89.0(3)	N(3)−Zr−C(2)	91.1(3)
N(1)−Zr−C(2)	101.7(4)	N(3)−Zr−C(4)	140.2(4)
N(1)−Zr−C(3)	112.4(3)	N(4)−Zr−C(1)	87.1(3)
N(1)−Zr−C(4)	114.4(3)	N(4)−Zr−C(2)	98.8(3)
N(2)−Zr−N(3)	87.3(3)	N(4)−Zr−C(3)	137.5(4)
N(2)−Zr−N(4)	99.2(3)	C(1)−Zr−C(2)	135.0(4)
N(2)−Zr−C(1)	167.3(3)	C(1)−Zr−C(3)	91.9(4)
N(2)−Zr−C(3)	90.9(3)	C(1)−Zr−C(4)	98.0(3)
N(2)−Zr−C(4)	93.1(3)	C(2)−Zr−C(3)	111.2(4)
C(2)−Zr−C(4)	110.4(4)	C(3)−Zr−C(4)	106.8(4)
C(1)−N(5)−C(5)	119.4(9)	C(2)−N(6)−C(7)	119.5(9)
C(1)−N(5)−C(6)	128.2(9)	C(2)−N(6)−C(8)	125.4(9)
C(5)−N(5)−C(6)	112.1(9)	C(7)−N(6)−C(8)	114.2(9)
C(3)−N(7)−C(9)	118.1(9)	C(3)−N(7)−C(10)	125.9(9)
C(9)−N(7)−C(10)	115.6(9)		

$NAr]_2\{\eta^2\text{-}C[Si(SiMe_3)_3]\text{=}NAr\}$ [2.200(4)−2.270(4) Å][9] and are consistent with dative Zr(IV)−N bond distances.[26] The Zr−C(4) (iminosilaacyl) bond [2.347(10) Å] is longer than the average Zr−C(amidino) bond [2.252(10) Å]. Such difference was also observed in $(Me_3CCH_2)Zr[\eta^2\text{-}C(CH_2CMe_3)\text{=}NAr]_2\{\eta^2\text{-}C[Si(SiMe_3)_3]\text{=}NAr\}$[9] and can be ascribed to the steric effect of the bulky $Si(SiMe_3)_3$ group. The Si−C(=N) bond distance [1.932(11) Å] in **7** is close to those in $(Me_3CCH_2)Zr[\eta^2\text{-}C(CH_2CMe_3)\text{=}NAr]_2\{\eta^2\text{-}C[Si(SiMe_3)_3]\text{=}NAr\}$ [1.921(5) Å],[9] $CpCp^*Zr\{\eta^2\text{-}C[Si(SiMe_3)_3]\text{=}NAr\}Cl$ [1.949(11) Å],[3e] $Cp_2Zr[\eta^2\text{-}C(SiPh_2Bu^t)\text{=}NPh]Cl$ (1.92 Å), and a silaacyl complex $Cp_2Zr(\eta^2\text{-}COSiMe_3)Cl$ [1.927(2) Å],[3a] but is longer than that found in the mono-insertion complex $(Me_3CCH_2)_3Zr\{\eta^2\text{-}C[Si(SiMe_3)_3]\text{=}NAr\}$ [1.897(4) Å].[9] The C−NMe_2 bond distances range from 1.341(12) to 1.365(13) Å and are between the C=N [1.270(12)−1.308(12) Å] and N−CAr bonds [1.417(13)−1.447(13) Å]. The short C−NMe_2 bonds in **7** suggest some degree of p−π bonding in the Me_2N−C=N moiety. This bonding feature is consistent with the fact that the sums of the angles around the Me_2N group are near 360°, and the ZrCN unit and Me_2N group are nearly coplanar.

(26) Chisholm, M. H.; Hammond, C. E.; Huffman, J. C. *Polyhedron* **1988**, *7*, 2515.

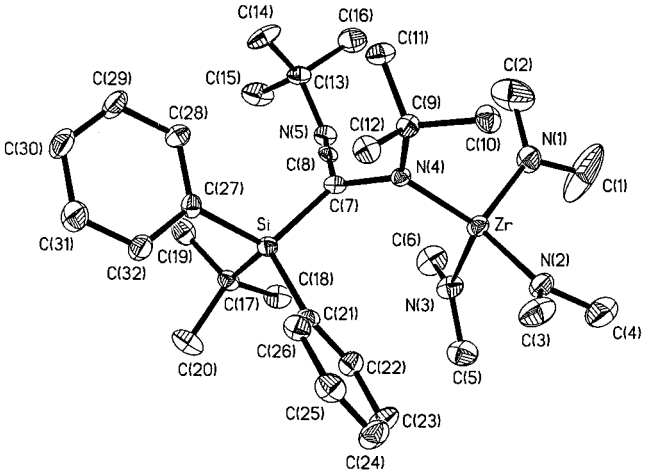

Figure 3. ORTEP drawing of $(Me_2N)_3Zr[NBu^tC(SiPh_2Bu^t)\text{=}C\text{=}NBu^t]$ (**12**), showing 35% thermal ellipsoids.

Table 4. Selected Bond Distances (Å) and Angles (deg) for 12

Distances			
Zr−N(1)	2.047(6)	N(4)−C(7)	1.457(7)
Zr−N(2)	2.044(6)	N(4)−C(9)	1.499(7)
Zr−N(3)	2.062(6)	C(7)−C(8)	1.335(9)
Zr−N(4)	2.067(5)	N(5)−C(8)	1.226(8)
Si−C(7)	1.888(6)	N(5)−C(13)	1.498(8)
Si−C(17)	1.922(7)	Si−C(21)	1.885(7)
Si−C(27)	1.899(7)		

Angles			
N(1)−Zr−N(2)	111.6(2)	C(7)−N(4)−C(9)	117.7(5)
N(1)−Zr−N(3)	101.8(2)	C(7)−C(8)−N(5)	170.7(7)
N(1)−Zr−N(4)	108.0(2)	C(8)−N(5)−C(13)	127.0(6)
N(2)−Zr−N(3)	103.1(2)	N(4)−C(7)−Si	124.9(4)
N(2)−Zr−N(4)	115.3(2)	C(8)−C(7)−Si	118.6(5)
N(3)−Zr−N(4)	116.4(2)	N(4)−C(7)−C(8)	115.8(6)
Zr−N(4)−C(7)	116.6(4)	C(7)−Si−C(17)	110.7(3)
Zr−N(4)−C(9)	125.5(4)	C(7)−Si−C(21)	107.7(3)
C(7)−Si−C(27)	113.0(3)	C(17)−Si−C(21)	111.3(3)
C(17)−Si−C(27)	104.7(3)	C(21)−Si−C(27)	109.5(3)

Molecular Structure of $(Me_2N)_3Zr[NBu^tC(SiPh_2Bu^t)\text{=}C\text{=}NBu^t]$ (12). An ORTEP drawing of the ketenimine complex **12** is shown in Figure 3. Selected bond distances and angles are listed in Table 4. The Zr atom is bonded to a ketenimine and three NMe_2 ligands to form a distorted tetrahedron; the bond angles between the N(4) atom of the ketenimine ligand and nitrogen atoms of the three amido ligands range from 108.0(2)° to 116.4(2)°. These angles are larger than the Si−M−N angles in $(Me_2N)_3ZrSi(SiMe_3)_3$ (**1**) [105.91(11)°] and $(Me_2N)_3TiSiPh_2Bu^t$ [104.6(2)°],[8] suggesting that the

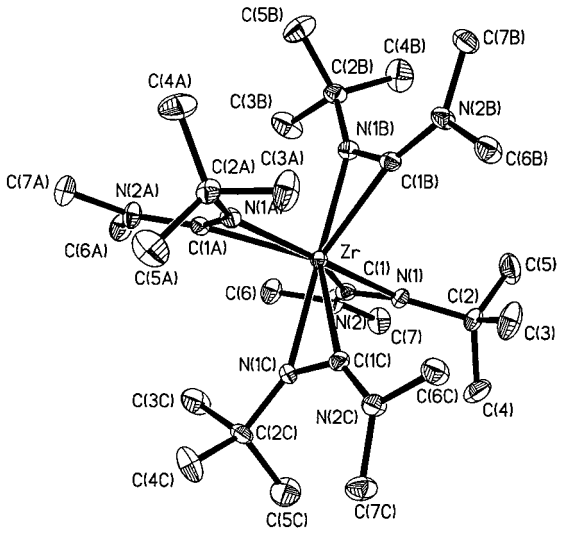

Figure 4. ORTEP drawing of $Zr[\eta^2\text{-}C(NMe_2)=NBu^t]_4$ (**13**), showing 35% thermal ellipsoids.

Table 5. Selected Bond Distances (Å) and Angles (deg) for 13

	Distances		
Zr−N(1)	2.235(3)	C(1)−N(1)	1.299(9)
Zr−C(1)	2.302(4)	C(1)−N(2)	1.356(8)
C(2)−C(3)	1.514(9)	C(2)−C(4)	1.529(7)
C(2)−C(5)	1.525(7)	N(2)−C(6)	1.439(8)
N(2)−C(7)	1.462(8)		
	Angles		
C(1)−Zr−N(1)	33.2(2)	Zr−C(1)−N(2)	156.8(4)
Zr−C(1)−N(1)	70.6(2)	Zr−N(1)−C(2)	145.5(5)
Zr−N(1)−C(1)	76.2(3)	N(1)−C(1)−N(2)	132.6(5)
C(1)−N(1)−C(2)	138.3(5)		

ketenimine ligand in **12** is more sterically demanding than the silyl ligands in **1** and $(Me_2N)_3TiSiPh_2Bu^t$. The Zr−N bonds range from 2.044(6) to 2.067(5) Å and are similar to those found in other known Zr(IV) amido complexes.[26,27] The C=C [1.335(9)] and C=N [1.226(8) Å] bond distances of the C=C=N moiety are similar to those found in other complexes containing a C=C=N functionality, such as [*p*-Bu^t-calix[4]-$(OMe)_2(O)_2$Zr-{N(Bu^t)C(Me_2)C(CNBu^t)N(Bu^t)}] [1.324(15) and 1.227-(14) Å],[16] $[(Me_3Si)N]_2Zr[Bu^tN{=}CMeC(=C=NBu^t)NBu^t]$ [1.345(4) and 1.205(4) Å],[24] $[(2,6\text{-}Pr^i_2C_6H_3)_2Cl_2]Ta[Bu^tN{=}CHC(=C=NBu^t)NBu^t]$ [1.338(6) and 1.206(5) Å],[23] [Zr-(TC-3,3){$NBu^tC(CH_2Ph)$=C=NBu^t}](BPh_4) [1.314(8) and 1.230(8) Å], and [Hf(TC-3,3){$NBu^tC(CH_2Ph)$=C=NBu^t}]-(BPh_4) [1.328(9) and 1.229(9) Å].[25]

Molecular Structures of $Zr[\eta^2\text{-}C(NMe_2)=NBu^t]_4$ (13) and $Zr[\eta^2\text{-}C(NMe_2)=NAr]_4$ (14). An ORTEP drawing of **13** is shown in Figure 4. Selected bond distances and angles are given in Table 5. The coordination sphere around the metal center is similar to that in **7**. However, the orientation of four η^2-amidino ligands is different from that in **7**. In **13**, four ZrCN units lie in two different, nearly perpendicular planes which bisect each other, and the carbon atoms in each plane are cis to one another. The Zr−N, Zr−C, C=N and C−N(amido) bond distances [2.235(3) 2.302(4), 1.299(9), and 1.356-(8) Å, respectively] are similar to those in **7**. An ORTEP drawing of **14** is shown in Figure 5. Selected bond distances and angles are listed in Table 6. The zirconium atom is coordinated by four η^2-amidino ligands, and the coordination sphere around it is similar to those in **7** and **13**. In **14**, the carbon atoms of η^2-amidino ligands in the same plane are trans to each other, as is observed in $Mo[\eta^2\text{-}C(NMe_2)=NAr]_4$.[17b] The orientation of the four η^2-amidino ligands in **14** is thus different from those in **7** and **13**. The average Zr−C and Zr−N bond distances are 2.276(13) and 2.232(11) Å, respectively, and are close to the corresponding values in **7** and **14**.

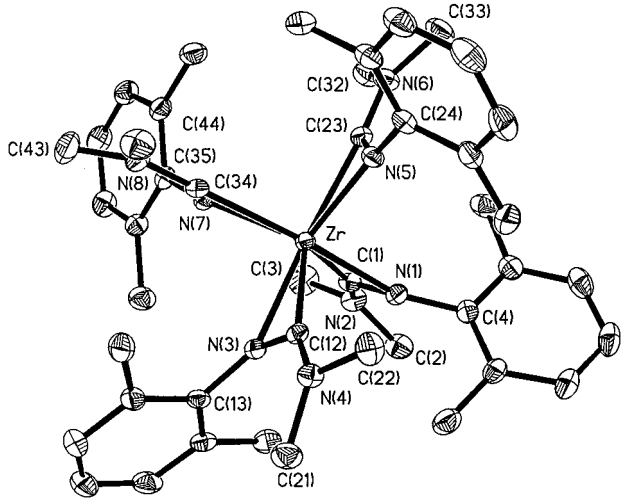

Figure 5. ORTEP drawing of $Zr[\eta^2\text{-}C(NMe_2)=NAr]_4$ (**14**), showing 35% thermal ellipsoids.

Table 6. Selected Bond Distances (Å) and Angles (deg) for 14

	Distances		
Zr−C(1)	2.263(4)	Zr−C(12)	2.267(3)
Zr−C(23)	2.282(4)	Zr−C(34)	2.303(4)
Zr−N(1)	2.267(3)	Zr−N(3)	2.259(3)
Zr−N(5)	2.206(3)	Zr−N(7)	2.194(3)
C(1)−N(1)	1.314(5)	C(12)−N(3)	1.306(4)
C(23)−N(5)	1.315(5)	C(34)−N(7)	1.317(5)
C(1)−N(2)	1.345(5)	C(12)−N(4)	1.348(4)
C(23)−N(6)	1.344(5)	C(34)−N(8)	1.344(5)
	Angles		
Zr−C(1)−N(1)	73.3(2)	Zr−C(12)−N(3)	72.9(2)
Zr−C(23)−N(5)	69.8(2)	Zr−C(34)−N(7)	68.5(2)
Zr−C(1)−N(2)	160.1(3)	Zr−N(1)−C(4)	152.0(2)
Zr−N(3)−C(13)	149.7(2)	Zr−C(12)−N(4)	158.8(3)
Zr−C(23)−N(6)	162.4(3)	Zr−N(5)−C(24)	148.2(2)
Zr−C(34)−N(8)	164.7(3)	Zr−N(7)−C(35)	149.6(2)
N(1)−Zr−N(3)	91.66(10)	N(1)−Zr−N(5)	93.48(11)
N(1)−Zr−C(12)	90.62(11)	N(1)−Zr−C(23)	88.67(12)
N(1)−Zr−C(34)	170.27(12)	N(3)−Zr−C(23)	171.80(12)
N(3)−Zr−C(34)	87.55(11)	N(5)−Zr−C(12)	104.51(12)
N(5)−Zr−C(34)	93.60(12)	N(7)−Zr−C(1)	102.78(13)
C(12)−Zr−C(34)	94.05(12)	C(23)−Zr−C(34)	93.49(12)

Influence of Steric Effects on Isocyanide Insertions into Zr−Amido and Zr−Silyl Bonds. Although isocyanide insertion into metal amido[17b,c] or metal silyl[3,18] bonds has been previously observed, the current work reports, to our knowledge, the first isocyanide insertions involving complexes containing both amido and silyl ligands. It is interesting to note that the first ArNC inserts into a Zr−N bond in the amido silyl

(27) (a) Brenner, S.; Kempe, R.; Arndt, P. *Z. Anorg. Allg. Chem.* **1995**, *621*, 2021. (b) Nugent, W. A.; Harlow, R. L. *Inorg. Chem.* **1979**, *18*, 2030. (c) Diamond, G. M.; Jordan, R. F.; Petersen, J. L. *J. Am. Chem. Soc.* **1996**, *118*, 8024. (d) Christopher, J. N.; Diamond, G. M.; Jordan, R. F.; Petersen, J. L. *Organometallics* **1996**, *15*, 4038. (e) Bradley, D. C.; Chudzynska, H.; Becker-Dirks, J. D.; Hursthouse, M. B.; Ibrahim, A. A.; Montevalli, M.; Sullivan, A. C. *Polyhedron* **1990**, *9*, 1423. (f) Wu, Z.; Dimmine, J. B.; Xue, Z. *Inorg. Chem.* **1998**, *37*, 2570.

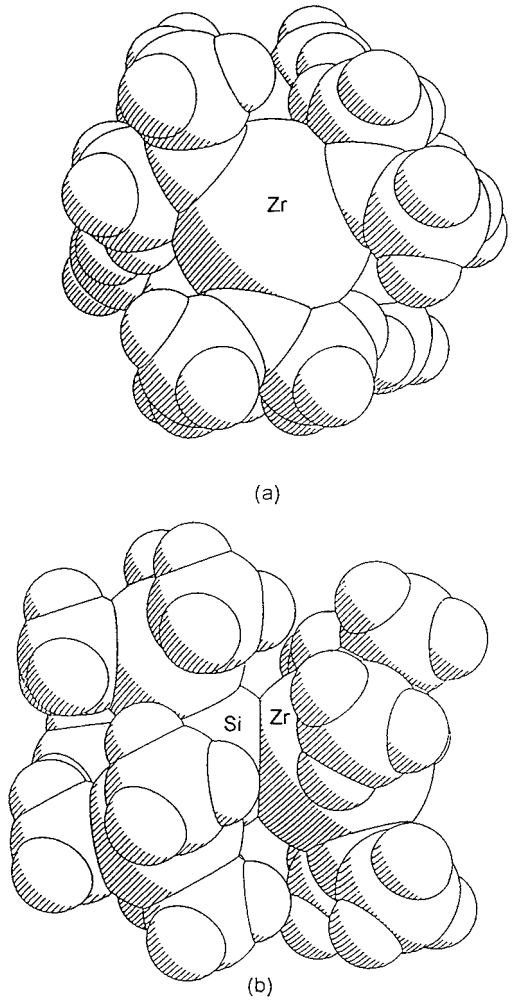

Figure 6. Space-filling drawings of $(Me_3CCH_2)_3ZrSi(SiMe_3)_3$:[9] (a) axial view along Zr−Si bond; (b) equatorial view.

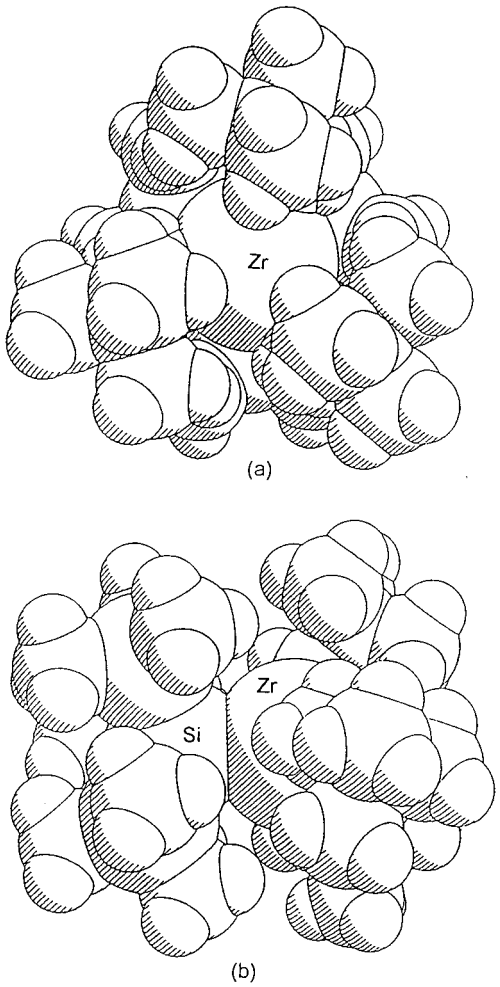

Figure 7. Space-filling drawings of $(Me_2N)_3ZrSi(SiMe_3)_3$ (**1**): (a) axial view along Zr−Si bond; (b) equatorial view.

complex $(Me_2N)_3ZrSi(SiMe_3)_3$ (**1**). In contrast, the first ArNC was found to insert exclusively into the Zr−Si bond in alkyl silyl complexes $(Me_3ECH_2)_3ZrSi(SiMe_3)_3$ (E = C, Si).[9] The reason for the difference in the reactivities of **1** and $(Me_3ECH_2)_3ZrSi(SiMe_3)_3$ (E = C, Si) toward isocyanide is not clear. Space-filling drawings of **1**[8] and $(Me_3CCH_2)_3ZrSi(SiMe_3)_3$[9] are shown in Figures 6 and 7, respectively. The largest open area of the zirconium atom in **1** for the attack of ArNC is between the amido ligands. We believe that the addition of the first isocyanide to the metal center in **1** may take place exclusively trans to the silyl ligand (Scheme 6) and that the reason for the amide migration is steric. The silyl ligand in **1** is not in a position to migrate onto the isocyanide carbon, and the amide migration is irreversible. An attack trans to the silyl ligand may also be preferred for the second equivalent of isocyanide. However, after two isocyanide insertions, the attack trans to the silyl ligand may become hindered, causing the third isocyanide attack to take place cis to the silyl ligand. In other words, the arrangement of the ligands in **1** directs the attack of the first and second isocyanide molecules to a position where only amide migration is feasible.

In $(Me_3CCH_2)_3ZrSi(SiMe_3)_3$,[9] the space between the alkyl ligands (trans to the silyl ligand, axial view) is much more crowded than that in **1**, perhaps making the

Scheme 6

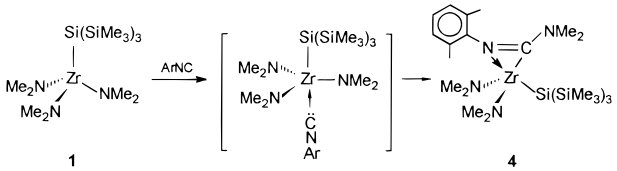

Ar = 2,6-dimethylphenyl

isocyanide addition between the alkyl and silyl ligands (cis to the silyl ligand, equatorial view) preferred (Scheme 1). This addition is followed by a migration of the bulky $Si(SiMe_3)_3$ group onto the isocyanide carbon. Tilley and co-workers have also observed the influence of the steric effects on CO insertions to the Zr−C and Zr−Si bonds in the reactions of CO with $Cp_2Zr(Me)Si(SiMe_3)_3$[3b] and $CpCp^*Zr(Me)Si(SiMe_3)_3$ ($Cp^* = \eta^5$-C_5Me_5).[3e] It was found that CO preferentially inserts into the Zr−C bond in $Cp_2Zr(Me)Si(SiMe_3)_3$[3b] and, in contrast, into the Zr−Si bond in the more bulky complex $CpCp^*Zr(Me)Si(SiMe_3)_3$ ($Cp^* = \eta^5$-C_5Me_5).[3e]

To confirm the influence of the steric effects on the insertion reaction of ArNC with $(Me_2N)_3ZrSi(SiMe_3)_3$ (**1**), we studied the reaction of $(Me_2N)_2[(Me_3Si)_2N]ZrSi(SiMe_3)_3$ (**3**) with ArNC. Compared to **1**, **3** contains a bulky $(Me_3Si)_2N$ ligand, which would block the open area between the amido ligands for the attack of ArNC. We indeed found that in the reaction of **3** with ArNC

Scheme 7

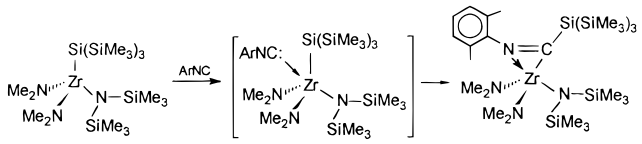

3 **9**

Ar = 2,6-dimethylphenyl

the first ArNC inserted into the Zr−Si bond to give a mono-insertion product **9** (Scheme 7). $(Me_2N)_3ZrSiPh_2Bu^t(THF)_{0.5}$ (**2**) also reacts with Bu^tNC to give exclusively the Zr−Si insertion products **11** and **12**, in contrast to the reactivity observed with $(Me_2N)_3ZrSi(SiMe_3)_3$ (**1**). THF coordination trans to the silyl ligand was found in the crystal structure of **2**,[8] which may prevent the ArNC approach to the Zr atom from this position. In addition, the exclusive formation of silyl insertion products **11** and **12** suggests that once the Zr−Si and Zr−N bonds are both available for the insertion of isocyanide, the silyl migration is more favorable than the amido migration, perhaps because the Zr−amide bonds are usually stronger than the Zr−silyl bonds.[28]

In conclusion, we have investigated the reactivities of Cp-free amido silyl complexes toward isocyanides. The current studies indicate that isocyanide insertion into Zr−silyl bonds is in general preferred and is often the first step in multi-insertion reactions. However, steric effects may play an important role in the insertion and may direct, for example, the first ArNC insertion to an M−amide bond in **1**. Steric congestion may also limit the number of isocyanide insertions, as observed in the inertness of complex **10** and **12** toward further isocyanide insertion.

Acknowledgment is made to the National Science Foundation (Grant CHE-9457368), the DuPont Young Professor Award, and the Camille Dreyfus Teacher-Scholar Award for financial support.

Supporting Information Available: Complete listings of crystallographic data for **7**, **12**, **13** and **14**. This material is available free of charge via the Internet at http://pubs.acs.org.

OM980979L

(28) King, W. A.; Marks, T. J. *Inorg. Chim. Acta* **1995**, *229*, 343.